

Optical characterization of nanostructured opal-C

DURÁN-MUÑOZ, H. A.†, SIFUENTES-GALLARDO, C., HERNÁNDEZ-ORTIZ, M., DÍAZ-CARRILLO, C., ULLOA-CAMPOS M., ORTIZ-HERNÁNDEZ A and GUTIÉRREZ-ALMARAZ G.”

Universidad Autónoma de Zacatecas, Departamento de Ingeniería Eléctrica, Av. Ramón López Velarde 801. Col. Centro, C.P. 98000. Zacatecas, Zac., México.

Universidad Politécnica de Zacateca, Carrera de Ingeniería Industrial. Plan del Pardillo S/N, Parque Industrial, Fresnillo, Zac. México.

Received: September, 8, 2017; Accepted: December, 15, 2017

Abstract

The emission of light from a thermally stimulated solid is called thermoluminescence (TL). The TL technique is a useful tool to characterize defects in materials. The aim of this work is realize a complementary TL study of synthetic opal-c reported on literature (Hernández-Ortiz *et. al.*, 2015; Hernández-Ortiz *et. al.*, 2012; Hernández-Ortiz *et. al.*, 2013), determining the kinetic parameters, which can be useful for photo transference applications, studies on defect creation, etc. Opal-C nanoparticles were synthesized by Stöber method. TL measurements of opal-c nanoparticles were carried out at room temperature using an automated Risø TL/OSL system model TL DA-20. Also, the Mckeever experiment was performed in order to know the peaks distribution, and was used a friendly glow curve deconvolution spreadsheet based on general order kinetic equation as a complementary technique to determine the kinetic parameters. Therefore, it is possible to carry out another level of synthetic Opal-C study, either to apply it in the medical sector, dosimetry, photo-transfer studies, archaeological dating, etc.

Thermoluminescence, Glow Curve Deconvolution and Opal-C Nanoparticles

Citation: DURÁN-MUÑOZ, H A†, SIFUENTES-GALLARDO, C, HERNÁNDEZ-ORTIZ, M, DÍAZ-CARRILLO, C, ULLOA-CAMPOS, M, ORTIZ-HERNÁNDEZ, A and GUTIÉRREZ-ALMARAZ, G. Optical characterization of nanostructured opal-C. ECORFAN Journal-Taiwan. 2017, 1-2: 1-5

† Researcher contributing as first author.

Introduction

The humanity is exposed directly and indirectly to opal, for example, some animals and plants contain opal as a cross-linking agent in a natural hydrated silica, with a crystal structure connective tissues (Iler, 1955 and 1979), and it is commonly used as semiprecious stone. Opal is type fcc and a direction [111] as the preferred orientation (Hernández-Ortiz *et. al.*, 2015; Golubev *et. al.*, 2002), and can be subdivided into three well defined structural groups: opal-CT, where the stacking sequence is apparently about 50% cristobalite and 50 % tridymite, and it is typically of volcanic origin (Hernández-Ortiz *et. al.*, 2012-B), it gives an X-ray diffraction pattern with markedly broad reflections, approximately at the positions of the strong lines of cristobalite; opal-C approximately 80 to 70% cristobalitic and 20 to 30% tridymitic; which is a well ordered form of the silicate and exhibit play-of-color of common opal (Jones and Segnit, 1971); play-of-color or noble opal is most known as opal-A (for amorphous), which is generally of sedimentary origin and it was found that there were anomalies in the relationship between water and hydroxyl content and certain physical properties, its classical localities are Australia and the Piauí State of Brazil (Graetsch *et. al.*, 1994; Fritsch *et. al.*, 2006).

Opal synthetic has a wide range of applications in different areas of knowledge, due to the ability to control the dimensions of the particle size; different particle sizes are required for different applications (Rossi *et. al.*, 2005). For example, silica nanoparticles, viewed as photonic crystal, are being developed as a host of biotechnological applications; one of them is the infiltration of biomolecules in photonic crystals to get improved luminescence spectra of DNA due to the possible formation of new photon-electron bound states.

Also, it is used on characterization of photonic materials performed by scattering matrix method (Reynolds *et. al.*, 1999). Recently, it has been proposed in dosimetry applications, due to bio-compatibility properties and an adequate response at high doses (Hernández-Ortiz *et. al.*, 2015; Hernández-Ortiz *et. al.*, 2012; Hernández-Ortiz *et. al.*, 2013).

However, an additional TL characterization on synthetic opal-C is necessary to perform. In order to characterize the defects associated to the overlapped peaks in a glow curve (electrical signal generated by TL technique). Each overlapped peak has peak parameters, I_m : maximum intensity of each peak, T_m : temperature in the maximum intensity and w : width of peak. Also, each defect has trap parameters, E : activation energy, s : frequency factor, b : order of kinetic and n_a : concentration of electron trapped. With the glow curve deconvolution technique, it is possible to obtain the trap and peak parameters.

The aim of this work is realize a complementary thermoluminescence characterization of synthetic opal-c reported on literature, determining the kinetic parameters, which can be useful in next works for photo transference applications, studies on defect creation, etc.

Methodology

In this work were used synthetic Opal-C samples, which were synthesized by Stöber method, consisting in the hydrolysis of tetraethyl-ortho-silicate (TEOS) using NH_3 as a catalyst and ethanol and acetone as solvent. The reaction was controlled in a Nalgene glass flask at room temperature. Synthetic opals underwent two thermal treatments aimed at strengthening the structure.

First annealing was fixed at 1000 °C for one day and second thermal treatment was given at 1150 °C for two days. According to the report of Beganskienė, the solution (TEOS, NH₃, H₂O and solvent) chemistry controls the reaction rate and particle size. The powdered samples were obtained by crushing the synthesized opal-c using an agate pestle. Then, TL measurements of opal-c nanoparticles were carried out at room temperature (~22 °C) using an automated Risø TL/OSL system model TL DA-20 equipped with a ⁹⁰Sr source beta (Figure 1) which delivers a 5 Gy min⁻¹ dose rate. All the TL measurements were performed using a linear heating rate of 5 °C s⁻¹ from 22 °C up to 510 °C, in an N₂ atmosphere.

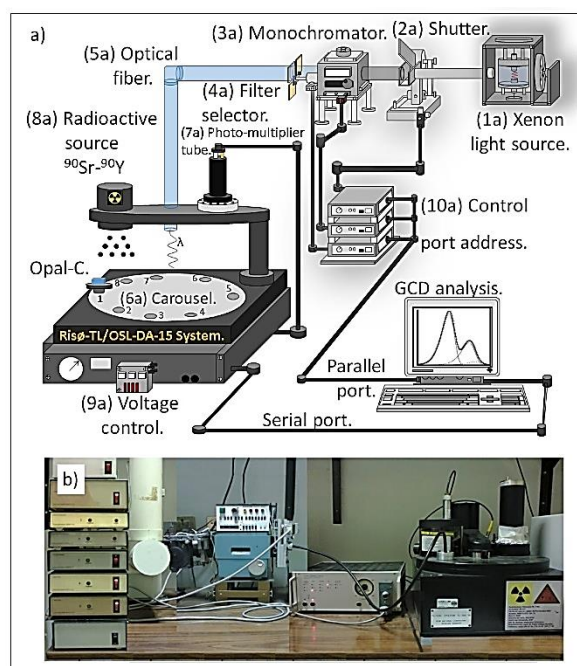


Figure 1. a) Diagram and b) experimental setup of luminescence system.

After of excitation, the carousel of Risø-TL/OSL-DA-15 system (Figure 1, 6a) is rotated to place the crystal below the photo-multiplier tube (Figure 1, 7a), and start a thermal stimulation producing light emission, which is detected with the photomultiplier tube.

The signal is processed by the computer and is represented as a glow curve. Finally, the McKeever experiment was performed with a thermal cleaning of $\Delta T = 5^\circ$ (T_{Stop}). Also, a friendly glow curve deconvolution spreadsheet (GCDS) based on general order kinetic equation was used as complementary technique to determine the kinetic parameters. This GCDS has been used to characterize other materials.

Results and Discussions

The McKeever experiment (Figure 2) reveals 3 ranges of emission, around of 50-270, 275-350 and 355-510 °C.

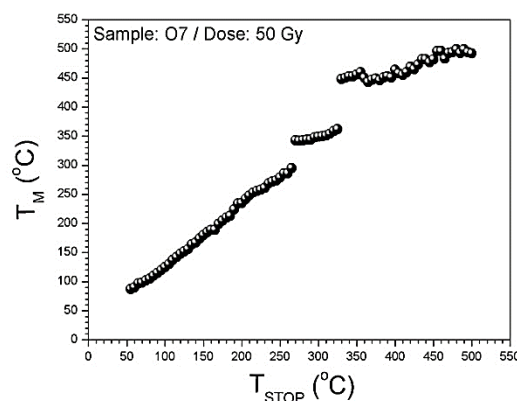


Figure 2. McKeever experiment graph (T_M - T_{STOP}), Opal-c sample exposed a dose of 50 Gy.

In the first temperature range (50-270 °C), 4 overlapped peaks are associated (1-4, Table 1), with activation energy very close to each other. These values support the hypothesis that the quasi-continuous distribution of traps occurs in this temperature range. In the second temperature range (275-350 °C), 2 overlapped peaks are associated (5-6, Table 1), with kinetic order values different from 1, which is supported by McKeever experiment (Figure 2).

In the third temperature range (355-510 °C), 2 overlapped peaks are associated (7-8, Table 1), with a large peak width and a kinetic of second order.

Using the GCDS, reported for the characterization of other materials (Muñoz *et al.*, 2014; Sánchez-Zeferino *et al.*, 2013), it was possible to identify the overlapped peaks in the experimental glow curve (Figures 3 and 4).

Using the simultaneously numerical fitting proposed in this work, it is possible to have evidence that the overlapped peaks obtained are associated with real values of the material.

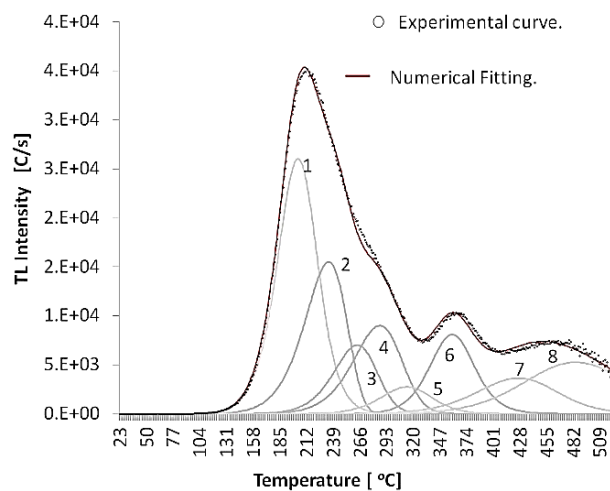


Figure 3. Glow curve deconvolution with a thermal treatment of 80 °C.

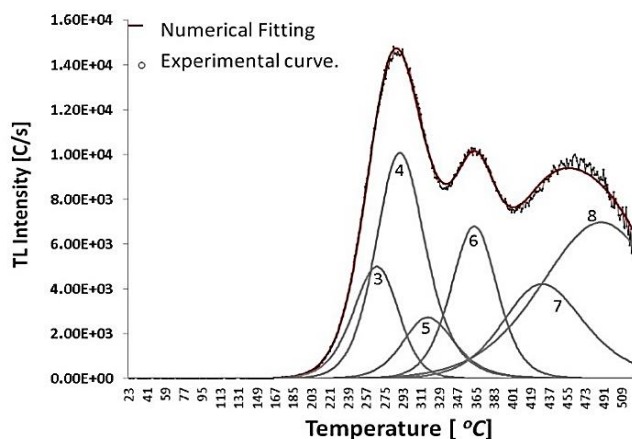


Figure 4. Glow curve deconvolution with a thermal treatment of 150 °C.

The simultaneously glow curve deconvolution process generates a FOM value (Figure of Merit) of 2.18. Normally, a FOM value below 5 is considered a good numerical fitting. The trap and peak parameters are presented in Table 1, with these parameters it is possible to identify the trapping states of opal-c.

Peaks	T_m [°C]	I_m [arb. u.]	w	E [eV]	s [s ⁻¹]	b
1	189	26041	46	1.1	5.47E+11	1.6
2	220	15497	51	1.0	1.57E+09	1.0
3	249	7035	50	1.2	6.04E+10	1.3
4	271	9020	56	1.1	5.41E+09	1.2
5	299	2762	59	1.3	1.35E+11	1.6
6	345	8106	51	1.9	1.77E+15	1.8
7	411	3666	94	1.2	4.14E+07	1.5
8	469	5258	135	1.2	7.41E+06	2.0

Table 1. Peak and trap parameters.

Conclusions

In this work the trap and peak parameters of Opal-C are presented for the first time. So, it is possible in other works to take to another level of the study of Synthetic Opal-C, either to apply it in the medical sector, for dosimetric, for studies of photo-transference, archaeological dating, etc. Particularly, The Mckeever experiment (Figure 1) reveals 3 ranges of emission, 50-270, 275-350 and 355-510 °C.

The peaks on low temperatures are generated by the quasi-continuous distribution of traps; while the other peaks correspond to kinetics of order different than 1 or general order. The results of this work serve as a reference for further physical studies.

Acknowledgements

The authors gratefully acknowledge the financial support for this work from PRODEP.

References

Boyko V., Dovbeshko G., Fesenko O., Gorelik V., Moiseyenko V., Romanyuk V., Shvets T. and Vodolazkyy P. (2011). *Mol. Cryst. Liq. Cryst.* 535, pp. 30–41.

Fritsch E., Gaillou E., Rondeau B., Barreau A., Albertini D. and Ostroumov M. (2006). *Journal of Non-Crystalline Solids* 352. Pp. 3957-3960.

Graetsch H., Gies H., Topalović I. (1994). *Physics and Chemistry of Minerals* 21, pp. 166-175.

Golubev V.G., Hutchison J.L. and Kosobukin V.A. (2002). *Journal of Non-Crystalline Solids* 1062, pp. 299–302.

Hernández-Ortiz M., Acosta-Torres L.S., Hernández-Padrón G. (2012). *BioMedical Engineering OnLine* 11, pp. 78-87.

Hernández-Ortiz M, Hernández-Padrón G, Bernal R, Cruz-Vázquez C, Vega-González M and Castaño V. (2012-B). *Digest Journal of Nanomaterials and Biostructures* 7(3), pp. 1297 – 1302.

Hernández-Ortiz M., Acosta-Torres L.S., Bernal R., Cruz-Vázquez C., Castaño V.M. (2013). *MRS Fall Proceeding 1530 mrsf12-1530-xx07-4*.

Hernández-Ortiz M, Hernández-Padrón G., Bernal R., Cruz-Vázquez C. and Castaño V. M. (2015). *International Journal of Basic and Applied Sciences* 4 (2), pp. 238-243.

Iler RK. (1955). New York: Cornell University Press.

Iler RK. (1979). New York: Wiley-Interscience.

Jones J.B., Segnit E.R. (1971). *Australian Journal of Earth Sciences* 18, pp. 57-68.

Masalov V., Sukhinina N., Emel'chenko GA. (2011). *Physics of the Solid State* 53. pp. 1135–1139.

Muñoz I., Brown F., Durán-Muñoz H., Cruz-Zaragoza E., Durán-Torres B., Alvarez-Montaña E. (2014). *Journal of Applied Radiation and Isotopes* 90, pp. 58–61.

Reynolds A., López-Tejiera F., Cassagne D., García-Vidal J., Jouanin C. and Sánchez-Dehesa. (1999). *J. Physical Review B.* 60, pp. 11422.

Rossi L., Shi L., Quina F. and Rosenzweig Z. (2005). *Langmuir* 21 pp. 4277-4280.

Sánchez-Zeferino R., Pal U., Meléndrez R., Durán-Muñoz H. and Barboza Flores M. (2013) Dose enhancing behavior of hydrothermally grown Eu-doped SnO₂ nanoparticles. *Journal of Applied Physics* 113 pp. 064306.